# Evidence for Dimerization of Dimers in $K^+$ Channel Assembly

LiWei Tu and Carol Deutsch
Department of Physiology, University of Pennsylvania, Philadelphia, Pennsylvania 19104-6085 USA

ABSTRACT Voltage-gated $K^+$ channels are tetrameric, but how the four subunits assemble is not known. We analyzed inactivation kinetics and peak current levels elicited for a variety of wild-type and mutant Kv1.3 subunits, expressed singly, in combination, and as tandem constructs, to show that 1) the dominant pathway involves a dimerization of dimers, and 2) dimer-dimer interaction may involve interaction sites that differ from those involved in monomer-monomer association. Moreover, using nondenaturing gel electrophoresis, we detected dimers and tetramers, but not trimers, in the translation reaction of Kv1.3 monomers.

## INTRODUCTION

Potassium ($K^+$) channels are formed from four identical subunits (MacKinnon, 1991; Schulteis et al., 1996), presumably organized with fourfold symmetry about the central pore (Li et al., 1994; Doyle et al., 1998). These tetramers are formed in the endoplasmic reticulum (Nagaya and Papazian, 1997) and reside in the plasma membrane as irreversibly formed channels (Panyi and Deutsch, 1996). Moreover, there is some evidence to show that monomers are recruited randomly from integrated monomer pools to form functional channels (Panyi and Deutsch, 1996). Although recognition domains (Li et al., 1992; Shen et al., 1993; Xu et al., 1995) have been identified in the cytoplasmic $NH_2$-termini of voltage-gated $K^+$ channels, and association sites within transmembrane segments of these channels have been implicated as contributing to intersubunit stabilization domains (Sheng et al., 1997), the mechanism by which tetramers form is still not known. Tetramers may form by stepwise sequential addition of monomers to form dimers, trimers, and, finally, tetramers (path A, Scheme I), and/or monomers may associate to form dimers, which dimerize to form tetramers (path B).

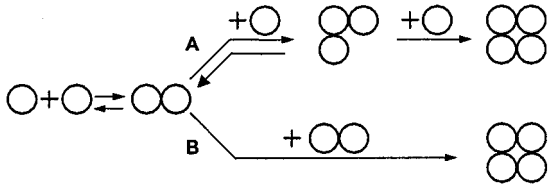


SCHEME I

In considering Scheme I, four key questions emerge: What are the relative contributions of these pathways? Does the trimer exist? Are the interaction sites identical along the reaction pathway (e.g., Does monomer-monomer association occur by the same mechanism as dimer-dimer association?)? What are the relative kinetics along each pathway? The answers have not been determined directly for voltage-gated $K^+$ channels, although other oligomeric structures provide some insights. Precedent for the dimer-dimer association pathway exists in the formation of acetylcholine receptor channels (Gu et al., 1991; Saedi et al., 1991; Blount et al., 1990; however, see Green and Claudio, 1993), the T-cell receptor (Manolios et al., 1991), and in the assembly of viral membrane proteins (Doms et al., 1993). In the first case, acetylcholine will not bind until a binding site is created by subunit oligomerization. Moreover, conformational changes and folding in intermediate oligomeric states are critical to the formation of new subunit recognition sites during assembly (Green and Claudio, 1993).

The goal of this work was to determine the relative contributions of these pathways to $K^+$ channel assembly and to determine whether the intermediate multimeric species have different interaction conformations. To do this we have used a variety of approaches. These include expression and suppression assays in *Xenopus* oocytes of Kv1.3 current generated from wild-type (WT) and mutant subunits injected as monomers or tandem dimers and trimers, a kinetic analysis of C-type inactivation for channel populations formed from coexpressed WT and mutant subunits, as well as nondenaturing gel electrophoresis. These studies support two conclusions. First, the dominant pathway in tetramer formation is dimerization of dimers, and the steady-state concentration of trimers is relatively low. Second, dimerization is likely to use interaction sites different from those involved in monomer-monomer association.

## MATERIALS AND METHODS

### Oocyte expression and electrophysiology

Oocytes were isolated from *Xenopus laevis* females (*Xenopus* I, Michigan) as described previously (Chahine et al., 1992). Stage V-VI oocytes were selected and microinjected with 3–15 ng cRNA encoding for Kv1.3, tandem dimers, and tandem trimers of Kv1.3. In the case of the chimera and AV-(WT-P), we used up to 40 ng cRNA to attempt to detect expression. The mole ratio of cRNA injected for Kv1.3 channel genes to putative suppressor genes (truncated $K^+$ channel gene, tandem gene, or chimera

*Received for publication 29 October 1998 and in final form 5 January 1999.*

Address reprint requests to Dr. Carol Deutsch, Department of Physiology, University of Pennsylvania, Philadelphia, PA 19104-6085. Tel.: 215-898-8014; Fax: 215-573-5851; E-mail: cjd@mail.med.upenn.edu.



0006-3495/99/04/2004/14 $2.00

1.3/3.1) was 1:1, 1:2, or 1:4, depending on the purpose of the experiment. Whenever a comparison was made, i.e., in the suppression and comparative expression experiments, we recorded the control and experiment from the same batch of oocytes from the same frog, always within a 2-h recording session. $K^+$ currents from cRNA-injected oocytes were measured with two-microelectrode voltage clamp using a OC-725C oocyte clamp (Warner Instrument Corp., Hamden, CT) after 15–72 h, at which time currents were 2–10 $\mu$A. This level of expressed current was optimal for observing suppression. Electrodes ($<1$ M$\Omega$) contained 3 M KCl. The currents were filtered at 1 kHz. The bath Ringer's solution contained (in mM) 116 NaCl, 2 KCl, 1.8 $CaCl_2$, 2 $MgCl_2$, and 5 HEPES (pH 7.6). The holding potential was $-100$ mV. Some data are presented as box plots, which represent the central tendency of the measured current. The box and the bars indicate 25–75 and 10–90 percentiles of the data, respectively. The horizontal line inside each box represents the median of the data. Other data sets are represented as mean $\pm$ SEM. To determine steady-state inactivation, we recorded from oocytes held for 2.5 s at voltages from $-100$ mV to $-10$ mV (10-mV steps), then at $-100$ mV for 0.1 ms, and finally at a test voltage of $+50$ mV for 45 ms. Between stimuli the oocytes were held at $-100$ mV for 50 s.

## Recombinant DNA techniques

Standard methods of plasmid DNA preparation, restriction enzyme analysis, agarose gel electrophoresis, and bacterial transformation were used. All isolated fragments were purified with "Geneclean" (Bio 101, La Jolla, CA), recircularized using T4 DNA ligase, and then used to transform DH5$\alpha^{TM}$ or XL1-blue competent cells (BRL, Gaithersburg, MD). The nucleotide sequences at the 5′ ends of all $NH_2$-terminal deletion mutants, at the 3′ ends of all C-terminal deletion mutants, and at the linkage sites between tandem constructs were confirmed by restriction enzyme analysis or by DNA sequence analysis (Sequenase Version 2.0 DNA Sequencing Kit; USB, Cleveland, OH).

## Plasmid constructs

Each tandem linkage lacks the first four amino acids in the amino terminus of the added subunit. Each construct containing a subunit that lacks the complete pore region ((Kv1.3-P), referred to as (WT-P) in the Results) contains the first five putative transmembrane segments and lacks the terminal half of the pore region through the carboxy terminus. The pGEM9zf(−)/Kv1.3-Kv1.3 tandem dimer (referred to as WT-WT in the Results) was made by isolating an *Eco*RI/*Mse*I blunt-end digested fragment (~1.8 kb) from pGEM9zf(−)/Kv1.3 and ligating it into partially *Sma*I-digested/*Eco*RI-digested pGEM9zf(−)/Kv1.3. The pGEM9zf(−)/Kv1.3-Kv1.3-Kv1.3 tandem trimer (referred to as WT-WT-WT in the Results) was made by ligating a partially *Pst*I-digested/*Hin*dIII-digested fragment (~2.2 kb) from pGEM9zf(−)/Kv1.3-Kv1.3 into partially *Pst*I-digested/*Hin*dIII-digested pGEM9zf(−)/Kv1.3-Kv1.3 (~5.8 kb). The pRc/CMV/Kv1.3-Kv1.3(A413V) (referred to as WT-AV in the Results) was made by ligating a partially *Apa*I/*Bst*EII-digested fragment (~2.8 kb) from pGEM9zf(−)/Kv1.3-Kv1.3 into partially *Apa*I-digested/*Bst*EII-digested CMV/Kv1.3(A413V) (Panyi et al., 1995). The pGEM9zf(−)/Kv1.3(A413V)-(Kv1.3-P) (referred to as AV-(WT-P) in the Results) was made by ligating an *Eco*RI/*Pml*I-digested fragment from pALTER-1/Kv1.3(A413V) into an *Eco*RI/*Pml*I-digested pGEM9zf(−)/Kv1.3(T1$^-$)-(Kv1.3-P), which was derived from ligation of a partially *Pst*I-digested/*Eco*RI-digested fragment from pGEM9zf(−)/Kv1.3(T1$^-$)-Kv1.3 into an *Eco*RI/*Pst*I-digested pGEM9zf(−)/Kv1.3(S3-S4-S5) (Tu et al., 1996). The pRc/CMV/Kv1.3-Kv1.3-Kv1.3(H399Y) (referred to as WT-WT-HY in the Results) was made by ligating a partially *Eco*NI-digested/*Bgl*II-digested fragment (~4.8 kb) from pRc/CMV/Kv1.3-Kv1.3-Kv1.3 into a *Eco*NI/*Bgl*II-digested pRc/CMV/Kv1.3(H399Y). The pRc/CMV/Kv1.3-Kv1.3-Kv1.3 was derived from an *Eco*RrI/*Hin*dIII-digested fragment isolated from pGEM9zf(−)/Kv1.3-Kv1.3-Kv1.3 and triple-ligated with an *Eco*RI/*Pvu*I-digested fragment and a *Pvu*I/*Hin*dIII-digested fragment, each of which were previously isolated from pRc/CMV. The pGEM9zf(−)/Kv1.3-Kv1.3-(Kv1.3-P) (referred to as WT-WT-(WT-P) in the Results) was made by ligating an *Eco*RI/*Pml*I-digested fragment from pGEM9zf(−)/Kv1.3(T1$^-$)-(Kv1.3-P) into partially *Pml*I-digested/*Eco*RI-digested pGEM9zf(−)/Kv1.3-Kv1.3-Kv1.3. The pGEM9zf(−)/Kv1.3-Kv3.1 chimera was made by ligating a *Bst*BI blunt end-digested/*Hin*dIII-digested fragment from pRc/CMV/Kv3.1 into an *Aat*II blunt end-digested/*Hin*dIII-digested fragment from pGEM/Kv1.3. The pRc/CMV/Kv1.3(H399Y) (referred to as HY in the Results) was made by mutating the histidine to tyrosine at position 399, using the PLATER-1 mutagenesis system (Promega, Madison, WI) and verified by DNA sequence analysis (Sequenase Version 2.0 DNA Sequencing Kit, USB). The mutant insert (1.8 kb) was cloned into a pRc-based plasmid containing a CMV eukaryotic promoter sequence (5.4 kb), yielding the pRc/CMV/Kv1.3(H399Y) plasmid. The S1-S2-S3 construct contains base pairs 441–941. It has 30 amino acids before S1 and 11 amino acids after S3. The S3-S4-S5 construct contains base pairs 843-1180, starting from S3 and ending 27 amino acids after S5 (Tu et al., 1996). Table 1 lists the above-mentioned constructs that were used to generate the data presented in the Results.

## In vitro translation

Capped cRNA was synthesized in vitro from linearized templates, using Sp6 or T7 RNA polymerase (Promega). Proteins were translated in vitro with [$^{35}$S]methionine (2 $\mu$l/25 $\mu$l translation mixture;~10 $\mu$Ci/$\mu$l Dupont/NEN Research Products, Boston, MA) in the absence of microsomal membranes for 60–180 min at 30°C (Fig. 2) or in the presence of canine microsomal membranes for the indicated times and temperatures (Fig. 6), in rabbit reticulocyte lysate, according to the Promega Protocol and Application Guide.

## Gel electrophoresis and fluorography

Electrophoresis was performed on a C.B.S. Scientific gel apparatus, using 7.5% SDS-polyacrylamide gels made according to standard Sigma protocols (Sigma Technical Bulletin, MWM-100). SDS in the sampling buffer, running buffer, and gel was 2%, 0.1%, and 0.1%, respectively. Native (nondenaturing) conditions were used in some experiments, in which case no SDS was present in the gel, and only 0.1% SDS was in the sampling buffer and running buffer. Gels were soaked in Amplify (Amersham Corp., Arlington Heights, IL) to enhance $^{35}$S fluorography, dried, and exposed to Kodak X-AR film at $-70$°C. Typical exposure times were $<36$ h. Quantitation of gels was carried out directly with a Molecular Dynamic PhosphoImager (Sunnyvale, CA).

**TABLE 1 Summary of Kv1.3 constructs**

| | |
|---|---|
| WT | Wild-type monomer |
| AV | Monomer with the A413V mutation in S6; speeds inactivation |
| HY | Monomer with the H399Y mutation in the pore; slows inactivation |
| WT-P | Monomer lacking terminal half of pore through C-terminus; nonfunctional |
| Chimera | Monomer containing S2 through C-terminus from Kv3.1; nonfunctional |
| WT-WT | Tandem dimer |
| WT-AV | Tandem dimer |
| AV-(WT-P) | Tandem dimer |
| WT-WT-WT | Tandem trimer |
| WT-WT-HY | Tandem trimer |
| WT-WT-(WT-P) | Tandem trimer |
| S1-S2-S3 | Truncated peptide Kv1.3 fragment |
| S3-S4-S5 | Truncated peptide Kv1.3 fragment |

## Data analysis

For experiments in which inactivation kinetics consisted of three exponentially decaying components, indicating three species of tetramers (e.g., Fig. 5, Scheme II), we fit the data in two steps. First, the three time constants were estimated at +50 mV, using the simplex algorithm (Clampfit, Axon Instruments). The fastest time constant ($\tau_1$) corresponds to a 2:2 WT:AV channel, the slowest ($\tau_3$) to a WT homotetramer (i.e., 4:0 stoichiometry), and the intermediate component to a 3:1 stoichiometry. The intermediate time constant ($\tau_2$) was calculated from $\tau_1$ and $\tau_3$ according to the cooperative model for C-type inactivation (Panyi et al., 1995). The mean values of these three time constants for 10–20 cells from the same batch of injected oocytes were used in the subsequent analysis of these cells.

The current decay in each cell was normalized to the value obtained 40 ms after the start of the depolarization and was fit to a mixture of three exponentially decaying components (Eq. 1) over an interval of 3.94 s, using a variable metric algorithm to minimize the sum of squared differences between data and theory:

$$I(t) = w_1 e^{-t/\tau_1} + w_2 e^{-t/\tau_2} + w_3 e^{-t/\tau_3} \tag{1a}$$

$$\sum_{i=1}^{3} w_i = 1.0 \tag{1b}$$

This analysis was used for the experiment in which WT-AV heterodimers were coexpressed with WT monomers (see Scheme II in the Results). For this model the weights in Eq. 1 can be expressed as

$$w_1 = w_d q^2 \tag{2}$$

$$w_2 = 2 w_d pq + w_m q \tag{3}$$

$$w_3 = w_d p^2 + w_m p \tag{4}$$

The probability that a dimer is a homodimer (WT-WT) formed from two WT monomers is $p$, and $q$ ($= 1 - p$) is the probability that a dimer is a tandem heterodimer (WT-AV). $w_d$ is the probability of channel formation by the dimer-dimer pathway from the dimerization of homo- and heterodimers (*pathway B* in Scheme II), and $w_m = 1 - w_d$ is the probability that tetramers form by the monomer addition pathway (*A* in Scheme II). The concentrations of each channel type will be proportional to the probabilities $p^2$ for the WT homotetramer (WT:AV of 4:0), $2pq$ for the WT:AV 3:1 heterotetramer, and $q^2$ for the WT:AV 2:2 heterotetramer. Note that the relative proportions of 2:2, 3:1, and 4:0 channel stoichiometries are 1:2:1 for a binomial distribution (Panyi et al., 1995), and the corresponding inactivation time constants are $\tau_1$, $\tau_2$, and $\tau_3$, respectively.

Equations 1–4 were tested for their ability to accurately determine values for $w_d$, $p$, and the fraction of each channel type formed ($w_j$; $j = 1$, 2, 3) by simulating data for known weights and time constants and then analyzing these data using Eqs. 1–4. The estimated values for $w_d$, $p$, and $w_j$ were correct to $\pm 0.001$.

We further verified Eqs. 1–4 by simulation of channel formation according to the kinetic model of Scheme II. Tetramers were assumed to be formed at a constant rate, $T$, and all reactions were assumed to be reversible, except for the final step, the formation of a tetramer, by either the monomer or dimer pathway. This last assumption is supported by the results of Panyi and Deutsch (1996). We further assumed that the rates of monomer and tandem dimer synthesis were constant. Strictly speaking, this assumption means that variations in the rate of monomer and tandem dimer synthesis are slower than the rate of assembly. After accounting for all species of reactants, the kinetic model can be expressed as a system of eight coupled first-order differential equations (Appendix). The solution was obtained by use of the Powell hybrid method, as implemented in the NAG Fortran Library (subroutine C05NBF; NAG, Downers Grove, IL). For arbitrary rate constants and rates of monomer and dimer synthesis, the fraction of tetramers formed by the dimer-dimer pathway, $w_d$, is given as

$$w_d = 1 - w_m = 1 - k_{13}[\text{Mon}][\text{Tri}]/T$$

where $k_{13}$ is the rate constant for the binding of a monomer to a trimer, [Mon] is the free concentration of WT monomers, and [Tri] represents the total concentration of all species of trimers. The relative fractions of each of the three possible tetramer species (Scheme II) are also obtained from the kinetic model. These fractions, when analyzed by Eqs. 1–4, produce an estimate of $w_d$ that agrees with the above simulated value within the limits of machine accuracy.

Note that the above model, although reversible in most steps, includes as a subset models in which all steps are irreversible. Our data show that tandem dimers contribute both subunits to tetramers (see Results and references therein), a necessary assumption for the above kinetic analysis.

## RESULTS

To assess the relative contributions of sequential monomer addition (A) versus dimer-dimer (B) pathways to tetramer formation (Scheme I), we used tandem multimers of Kv1.3 in which specific subunits were functionally tagged with mutations or deletions (see Table 1). It was first necessary to characterize the currents obtained from monomer (WT), wild-type tandem dimer (WT-WT), and wild-type tandem trimer (WT-WT-WT). As shown in Fig. 1, each construct expressed well in oocytes and produced currents that were similar with respect to current-voltage curves (*B*), steady-state inactivation curves (*C*), and inactivation time constants (*D*). For the currents shown in Fig. 1 *A*, different molar amounts of cRNA were injected for each plasmid to give approximately the same level of current for the same postinjection time. To verify that tandem cRNA was capable of being translated completely, we translated WT, WT-WT, and WT-WT-WT cRNA in rabbit reticulocyte lysate. The translation reactions produced proteins that appeared as bands at 60, 110, and 170 kDa, respectively, on SDS-PAGE (Fig. 2), consistent with the predicted molecular weights for WT, WT-WT, and WT-WT-WT.

### Contributions of concatenated subunits

#### *Tandem dimers donate two subunits per tandem*

A strategy for confirming complete translation of tandem dimers and trimers in vivo is to construct and characterize concatenated Kv1.3 subunits that contain a functionally tagged mutant subunit in any tandem position. For example, a mutation of Kv.1.3 that replaces $Ala^{413}$ in the beginning of the sixth transmembrane segment with valine (AV) causes a ~50-fold increase in the rate of inactivation at +50 mV (Panyi et al., 1995). If a tagged tandem subunit is not completely translated, is unstable, or does not contribute to the tetramer, then the resulting channel will lack the hallmark effect of the mutant on the inactivation kinetics. Alternatively, a tandem containing a nonfunctional subunit will also be diagnostic for expression and subunit participation. If the nonfunctional subunit is donated to the tetramer, then it will competitively inhibit a functional subunit from participating in formation of the channel, and the

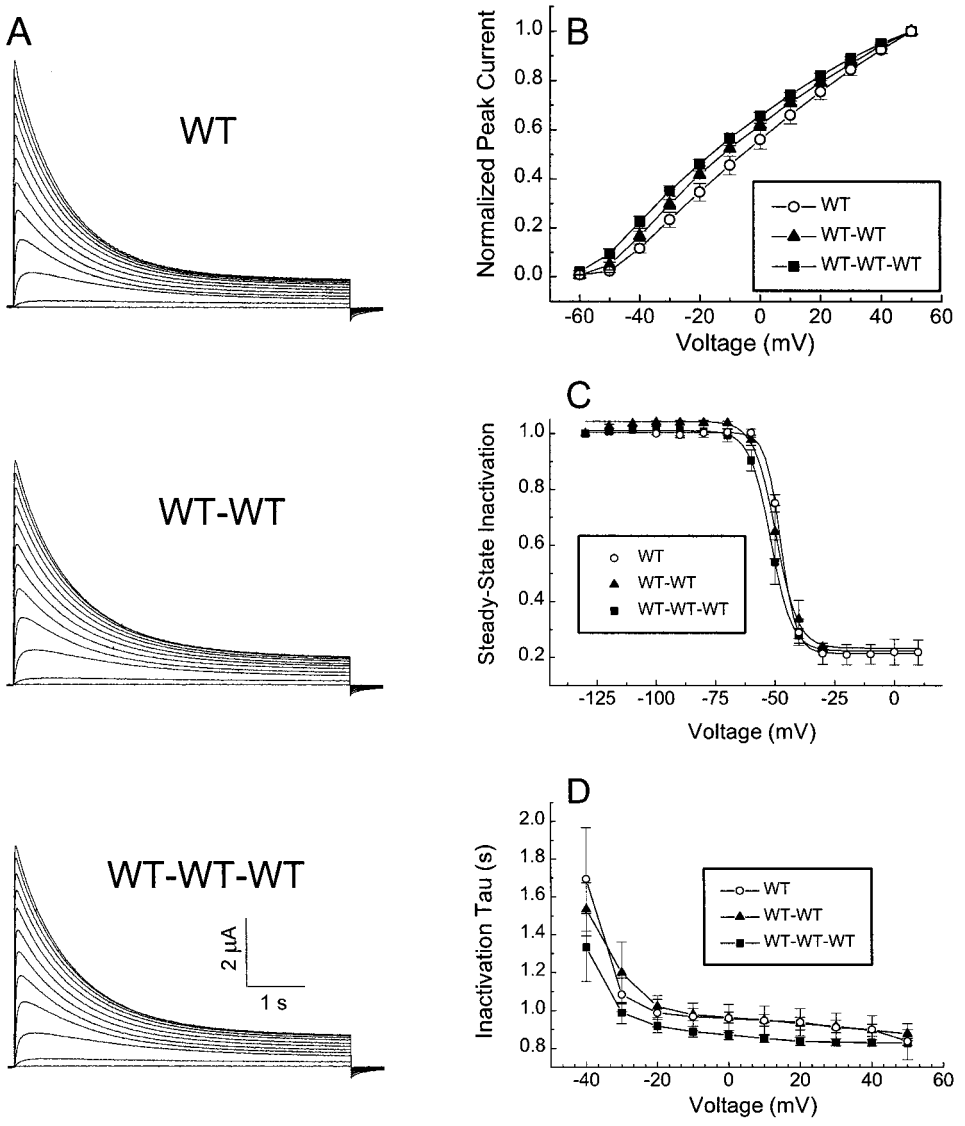


FIGURE 1 Characterization of currents derived from the expression of WT, WT-WT tandem dimer, and WT-WT-WT tandem trimer. Oocytes were injected with WT, WT-WT, or WT-WT-WT cRNA (8, 10, 15 ng per oocyte, respectively), and currents were recorded as described in Materials and Methods. The quantities of cRNA injected were empirically determined to give ~ similar ranges of current. (*A*) Currents elicited by steps from a holding potential of −100 mV to voltages between −60 and +50 mV in 10-mV increments. The average current at +50 mV was 6.5, 6.9, and 4.2 μA for WT, WT-WT, and WT-WT-WT, respectively. (*B*) Current versus voltage for the data shown in *A*. (*C*) Steady-state inactivation versus voltage for cells held at the indicated voltages for 2.5 s at voltages from −130 mV to −10 mV (10-mV intervals), then at −100 mV for 0.1 ms, and finally at a test voltage of +50 mV for 45 ms. Between stimuli the oocytes were held at −100 mV for 50 s. The normalized peak current at each test voltage was averaged to give the mean ± SEM for five cells. The midpoints of the steady-state inactivation curves were −48, −50, and −51 mV, respectively. (*D*) Inactivation time constant versus voltage for currents elicited by steps from a holding potential of −100 mV to voltages between −40 and +50 mV in 10-mV increments. For each voltage, inactivation time constants, derived from the best fit of a single-exponential function to the decay of the current, were averaged to give the mean ± SEM for four cells.

resultant level of current expressed will be suppressed. If only one of the two subunits in the tandem is donated to the channel, then a small but finite amount of current will be expressed, derived from functional homotetramers (i.e., structural octamers). If the two subunits of the tandem are donated simultaneously to the same channel, then all resultant channels will be nonfunctional and there will be no detectable current. Such suppression strategies have been used to probe for putative intersubunit interaction sites in Kv1.3 (Tu et al., 1995, 1996; Panyi and Deutsch, 1996; Sheng et al., 1997). In the following experiments, we have used these strategies to examine subunit participation in channel formation.

We constructed a tandem dimer containing a full-length Kv1.3 AV subunit in the first position of the dimer and in the second position, a truncated Kv1.3 WT subunit that lacks the pore through the carboxy terminus (WT-P). Oocytes expressing this AV-(WT-P) tandem were clamped at a holding potential of −100 mV and stepped to +50 mV for 200 ms. Only background currents (0.14 ± 0.01 μA, $n = 5$)

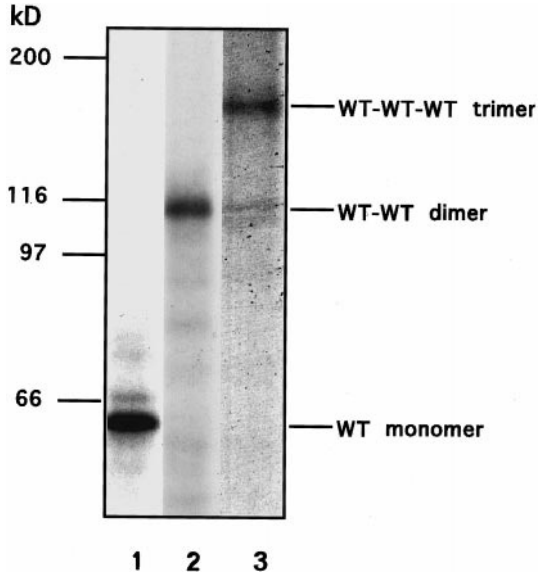


FIGURE 2 In vitro translation of WT, WT-WT, and WT-WT-WT Kv1.3. cRNA for WT (*lane 1*), WT-WT (*lane 2*), and WT-WT-WT (*lane 3*) were translated and labeled with [$^{35}$S]methionine as described in Materials and Methods and electrophoresed using a 7.5% SDS-polyacrylamide gel.

were recorded from oocytes injected with 15 ng/oocyte of AV-(WT-P). This was true even for higher cRNA concentrations (up to 40 ng/oocyte) and for holding potentials more negative than −100 mV, whereas control oocytes injected with 15 ng/oocyte of a WT-AV tandem dimer gave ≥10 $\mu$A of current for the same protocols, indicating that current could have been detected if functional channels were present in the membrane. Because both species of dimer are translated completely and likely form tetramers on their own (see Figs. 3 and 8), these results suggest that both

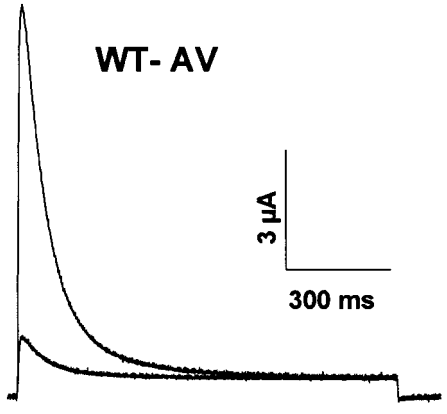


FIGURE 3 Expression of WT-AV current in oocytes. Oocytes were injected with cRNA for WT-AV tandem dimer, and recordings were made 24 h postinjection. Currents were elicited by a step to +50 mV from a holding potential of −100 mV. The best fit of a single-exponential function to the decaying phase of the current gives an inactivation time constant of 81 ms. The second current trace is lower than the first and was obtained 2 s after the first pulse.

subunits are contributed to the tetramer by the tandem dimer.

If this is so, then a 2:2 WT:AV stoichiometry is predicted to occur upon expression of WT-AV. Fig. 3 shows the current elicited by two 1100-ms depolarizations from −100 mV to +50 mV from an oocyte injected with WT-AV. The interpulse interval was 2 s. The smaller current during the second depolarization is a consequence of a slow recovery from inactivation. Similar current levels were elicited for the first pulse, using holding potentials of −100, −120, and −140 mV; i.e., no inactivation occurred at holding potentials from −140 to −100 mV. The decay of WT-AV is markedly enhanced compared to that obtained for an identical depolarization of an oocyte expressing WT-WT current (Fig. 1 *A*). A single-exponential function was fit to the decay to give an average time constant of 83.0 ± 1.3 ms ($n$ = 6). According to the analysis of Panyi et al. (1995), time constants for heterotetramers can be calculated from the measured time constants for the WT homotetramer, the AV homotetramer, and the equation $\tau_m = \tau_{WT}/F^m$, where $m$ is the number of mutant subunits in the heterotetrameric channel and $F$ is a cooperativity factor derived from the homotetramers. The measured time constant, 83 ms, is consistent with the time constant calculated for a subunit stoichiometry of 2WT:2AV. Moreover, the recovery from inactivation is slowed markedly (*smaller current trace* in Fig. 3) compared to WT-WT. For the same depolarization duration, the fractional recovery was only 5.6 ± 0.6% ($n$ = 6) for WT-AV compared to 43.4 ± 2.8% ($n$ = 6) for WT-WT (data not shown). These results demonstrate that the subunit in the second position of the tandem (AV) was translated and was stable. Moreover, these results argue that most of the channels are formed from two WT-AV dimers. If, for example, four tandem dimers each donated one subunit at random, then the predicted channel population would be heterogeneous (i.e., composed of five channel stoichiometries, each contributing a unique time constant), contrary to the observed results.

Taken together, these experiments suggest that two dimers are able to form a tetramer, that they do so by contributing two subunits per tandem to the tetramer, and that an octameric structure is unlikely. Similar conclusions have been made previously for tandem dimers of voltage-gated and cyclic nucleotide-gated channels (e.g., Heginbotham and MacKinnon, 1992; Ogielska et al., 1995; Panyi et al., 1995; Liu et al., 1996; Liu et al., 1998; however, see McCormack et al., 1992).

### *Tandem trimers donate two subunits per tandem*

Although tandem dimers can tetramize via dimer-dimer interactions, it is not clear whether this is a general mode of tetramer formation regardless of the subunit source, or a specific mode for tandem dimers. For instance, how many subunits of a tandem trimer participate in the formation of a channel tetramer? To address this issue, we constructed the trimer WT-WT-(WT-P), which contains a truncated, non-

functional subunit in the C-terminal position, and compared the currents elicited from oocytes separately injected with an equal cRNA molar concentration of WT-WT-WT or WT-WT-(WT-P). If tandem trimers behave like tandem dimers, i.e., donate two subunits per tandem, then we expect to detect some current from WT-WT-(WT-P). If only the first subunits of each trimer associate to form a channel, then WT-WT-WT and WT-WT-(WT-P) should give identical currents. If a trimer is a structural part of the channel, preferentially donating all three of its subunits to a channel, then we do not expect to detect current from WT-WT-(WT-P). However, WT-WT-(WT-P) gave a median current of 2.71 $\mu$A ($n = 8$), which is only 27% of the median current level (9.98 $\mu$A; $n = 8$) measured for WT-WT-WT. Similar results were obtained for comparisons made at 24 and 48 h postinjection. These results suggest that in a tandem trimer the third position (C-terminus) is translated and may participate in channel assembly. Moreover, a tandem trimer is more likely to donate two rather than three subunits to a tetrameric channel.

Similar conclusions may be made using another tandem trimer, WT-WT-HY, in which the C-terminal subunit, HY, contains a tyrosine instead of $His^{399}$ at the outer mouth of the pore. This mutation slows the kinetics of C-type inactivation (Busch et al., 1991; Panyi and Deutsch, 1997). We expressed this tandem trimer to determine whether the mutant subunit in the C-terminal position of the trimer was capable of contributing to the population of functional tetramers. Fig. 4 shows currents obtained at a series of voltages for oocytes injected with WT-WT-WT trimer (*left*), HY monomer (*middle*), and WT-WT-HY trimer (*right*). Note the different time scales for the depolarizations. A comparison of the inactivation kinetics of WT-WT-HY with those of WT-WT-WT indicates that the C-terminal subunit position of the trimer was donated to the tetrameric channel because the inactivation kinetics of the channel formed from WT-WT-HY were markedly slowed. For WT-WT-WT, the inactivation time constant at +50 mV for a 20-s depolarization was 0.951 s, much faster than that of the HY homotetramer. (The HY homotetramer has complicated inactivation kinetics, with more than two time constants (unpublished). However, the major components, representing ~90% of the decay, are much slower (>30-fold at +50 mV) than the inactivation time constant of WT channels. The complicated kinetics preclude the possibility of determining the exact stoichiometry of HY/WT heterotetramers.) For the WT-WT-HY, ~50% of the current decay had a time constant of 0.9 s, comparable to that of the WT homotetramer. This indicates that not all three subunits of a trimer could always be contributing to the channel. Given the conclusions from the previous experiments, these results suggest that some channels arise from the donation of two WT subunits per tandem trimer. Therefore, a dimer-dimer pathway is likely to be a major route in channel assembly from tandem constructs.

## Inactivation kinetics reveal that a dimer-dimer pathway predominates

The above expression and suppression experiments suggest that a dimer-dimer pathway for assembly of Kv1.3 exists. However, these experiments do not address whether a dimer-dimer pathway or a sequential monomer addition pathway is favored when monomers are present. To determine which pathway predominates in tetramer formation, our strategy was to analyze the inactivation kinetics resulting from coexpression of two species that would produce different channel populations, depending on the pathway by which they formed channels. For example, as shown in Scheme II for coexpression of WT-AV tandem dimer with WT monomer, assuming that each tandem dimer donates two subunits (shown above and in references therein) and the association of subunits is random (Panyi et al., 1995), three channel stoichiometries of WT:AV subunits are possible: 4:0, 3:1, and 2:2. The monomer addition pathway (A)

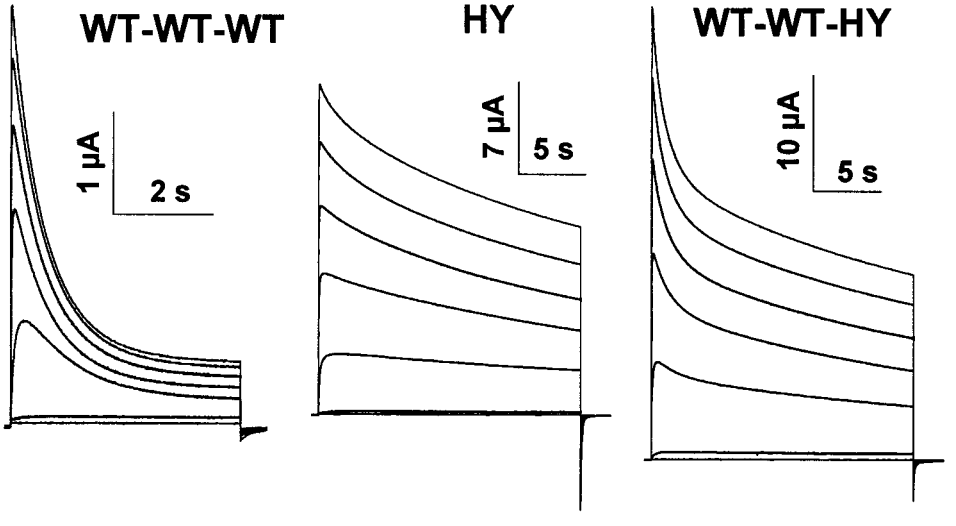


FIGURE 4 Expression of WT-WT-HY current in oocytes. Oocytes were injected separately with cRNA for WT-WT-WT tandem trimer (*left*), HY monomer (*middle*), or WT-WT-HY tandem trimer (*right*), and recordings were made 15–48 h postinjection. Currents were elicited by a step from a holding potential of −100 mV to voltages between −70 mV and +50 mV in 20-mV increments for a pulse duration of 60 s.

can only produce channels with 4:0 and 3:1 stoichiometries, whereas the dimer-dimer pathway (B) produces all three types of channels: 4:0, 3:1, and 2:2.

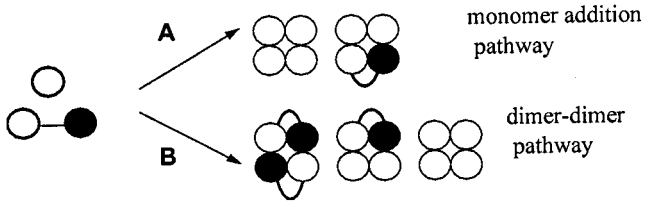


SCHEME II

Consequently, the overall distribution of the three channel types will be the sum of the two pathways and will depend on the relative contributions of each of the pathways. We coexpressed WT-AV tandem dimer with WT monomer and fit the inactivation kinetics of the current elicited at +50 mV by a weighted sum of three exponentials (Eq. 1). The weights (Eqs. 2–4) represent the fraction of each tetrameric species in Scheme II. We tested the validity of these equations by using simulated data as described in Materials and Methods and the Appendix.

Equations 1–4 were used to fit inactivation kinetics from 10 cells in each of three cases in which the cRNA mole ratios of WT-AV to WT monomer were 1:1, 1:3, and 1:5. A representative current trace for each case, along with the best fits, is shown in Fig. 5. The probability that a dimer is a homodimer (WT-WT) formed from two WT monomers is $p$, and $w_d$ is the probability of channel formation by the dimer-dimer pathway from dimerization of homo- and heterodimers (*pathway B*, Scheme II). The average $p$, $w_d$, and fractions of each channel stoichiometry, $w_j$, obtained for each mole ratio are given in Table 2. The fits are quite good, as judged visually from Fig. 5 and from the calculated sums of squared errors in Table 2. The values of $w_d$ indicate that the dominant pathway leading to tetramer formation is the dimer-dimer pathway, even at high relative monomer concentration. With increasing mole ratios of monomer cRNA compared to tandem dimer, the average fraction of channels (regardless of how they were formed) that are WT homotetramers, a reflection of total monomers synthesized, increased from 0.17 ± 0.02 to 0.69 ± 0.03 (mean ± SEM, Table 2). In these cases, the fractions of homodimer ($p$) were 0.32 ± 0.02, 0.74 ± 0.02, and 0.83 ± 0.02, and $w_d$ was 0.73 ± 0.06, 1.00 ± 0.00, and 1.00 ± 0.00 (mean ± SEM), respectively. These results also suggest that at relatively high monomer synthesis rates, homodimers form quickly and preferentially compared to trimer formation between a monomer and a heterodimer. Thus the dimer-dimer pathway dominates, even when monomers and tandem dimers are present. This analysis does not depend on the mechanism by which a tandem interacts with a dimer (be it a tandem dimer or a homodimer formed from two monomers), but rather on the fact that the tandem does interact with a dimer.

## A dimer and a tetramer, but not a trimer, are detectable

Given these results, we expect to detect monomers, dimers, and tetramers, but no trimers, when WT Kv1.3 is translated in the presence of microsomal membranes. Translation reaction mixtures were centrifuged through a sucrose cushion to isolate membrane vesicles because we have previously shown that association of an $NH_2$-terminally deleted Kv1.3 and Kv1.3 peptide fragments occurs in the membrane (Sheng et al., 1997) in a time-dependent manner (A time dependence has also been shown for Kv1.1 and Kv1.4 association (Deal et al., 1994).) Solubilization of membrane-integrated Kv1.3 in dodecylmaltoside ($C_{12}M$) at 4°C, followed by relatively nondenaturing (see Materials and Methods) gel electrophoresis, gave the results shown in Fig. 6. The first three lanes contain calibration bands derived from WT monomer, WT-WT tandem dimer, and WT-WT-WT tandem trimer, respectively, at their correct molecular weights. Lanes 4–6 and 7–8 contain products derived from the translation of WT monomer at 20°C and 24°C, respectively, for the indicated times. These samples show bands at the appropriate molecular weights for mono-

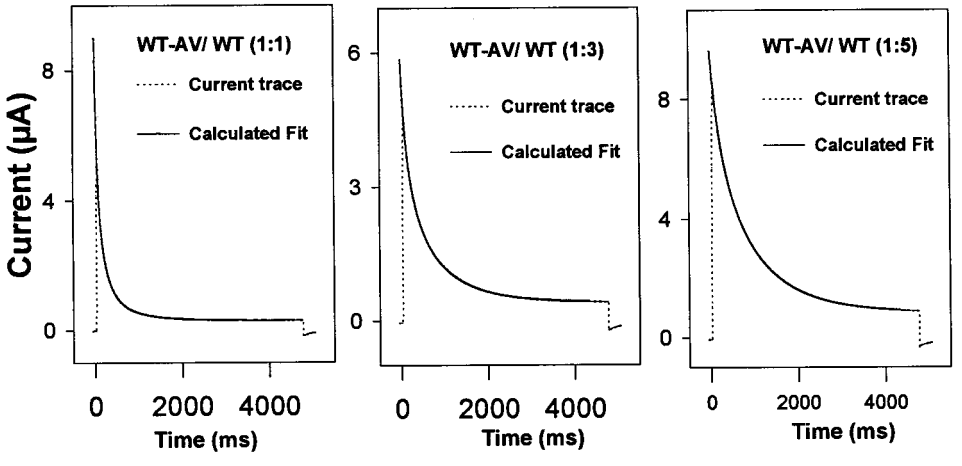


FIGURE 5 Coexpression of WT-AV and WT subunits in oocytes. Oocytes were coinjected with WT-AV and WT subunits in cRNA mole ratios of either 1:1 (*left*), 1:3 (*middle*), or 1:5 (*right*), respectively. Recordings were made 20–48 h postinjection. Currents were elicited by a step to +50 mV from a holding potential of −100 mV (·····). The decay of the current was fit according to Eqs. 1–4 in the Results (——). The best fits gave $w_d$ and $p$ values of 0.62 and 0.31 for 1:1, 1.00, and 0.75 for 1:3, and 1.00 and 0.84 for 1:5 cRNA mole ratios.

**TABLE 2 Summary of kinetic analysis of coexpression of WT monomers and WT-AV tandem dimers**

| WT-AV:WT cRNA | $p$ | $w_d$ | $w_1$ 2WT:2AV | $w_2$ 3WT:1AV | $w_3$ 4WT | SSE |
|---|---|---|---|---|---|---|
| 1:1 | 0.32 ± 0.03 | 0.73 ± 0.06 | 0.32 ± 0.02 | 0.51 ± 0.01 | 0.17 ± 0.02 | 0.008 ± 0.003 |
| 1:3 | 0.74 ± 0.02 | 1.00 ± 0.00* | 0.07 ± 0.01 | 0.37 ± 0.02 | 0.56 ± 0.03 | 0.026 ± 0.006 |
| 1:5 | 0.83 ± 0.02 | 1.00 ± 0.00* | 0.03 ± 0.004 | 0.28 ± 0.02 | 0.69 ± 0.03 | 0.018 ± 0.004 |

$p$ is the estimated fraction of homodimers (Eqs. 2–4) at steady state, and $1 - p$ is the fraction of WT-AV heterodimers. $w_j$ is the fraction of each channel type that has WT:AV subunit stoichiometries of 2:2, 3:1, and 4:0, respectively, for $j = 1, 2, 3$. $w_d$ is the fraction of tetramers that were assembled using a dimer-dimer interaction. Note that all (2WT:2AV) tetramers are made by the dimer-dimer pathway. Ten cells were used for each mole ratio of cRNA. Values are mean ± SEM. SSE is the sum of squared differences between data and theory.

*The value of $w_d$ is constrained to a maximum of unity and a minimum of zero. In the case of cRNA ratios of 1:3 and 1:5, all cells produced an estimate of $w_d > 0.99$.

mer, dimer, and tetramer. No trimer was detected, even with longer exposure times. This experiment was also performed at 30°C for 3 h, but no trimer could be detected (data not shown). The diffuse dimer bands could represent different dimers with different mobilities.

Fig. 6 also indicates that the relative amounts of dimers and tetramers are sensitive to the duration and temperature of the translation reaction. This is consistent with previous results (Sheng et al., 1997) showing that the rate-limiting step in complex formation is the association of membrane-integrated protein. Long times are required because of the low efficiency of protein integration into the membrane in the rabbit reticulocyte lysate system and consequent low membrane concentration of protein. The kinetics of tetramer assembly, being a function of Kv1.3 concentration in the membrane, are therefore slow. Using pulse-chase experiments, we have determined that tetramers are stable in $C_{12}M$ at 4°C over a 19-h period (data not shown). However, some fraction of tetramers may dissociate in the sampling buffer, which contains 0.1% SDS (to minimize smearing on gels that occurs when SDS is absent), and/or during subsequent electrophoresis. Despite these possibilities it is clear that the tetramer increased between 8 and 24 h, whereas the dimer concentration decreased over this time period (Fig. 6 *B*). The inset normalizes the tetramer to the dimer in each lane, thereby obviating potential artifacts due to unequal total protein in each sample.

Together, these data suggest that the distribution of multimers shifts toward the tetramer with time, and that the detected dimer could not have been formed exclusively from dissociation of tetramers in the sampling buffer or gel. Furthermore, these results are consistent with dimers forming relatively quickly and then dimerizing more slowly to form tetramers. The purpose of the experiments shown in Fig. 6 was to detect trimers. If we had detected trimers, it would have meant that the monomer pathway exists. No detection means that if trimers exist, they are short-lived for any of several reasons. The trimer could be unstable in detergent or during electrophoresis, and/or transient in the membrane during assembly. A lack of detected trimer does not preclude trimer formation along a monomer addition pathway.

## Dimer interaction sites differ from monomer-monomer interaction sites

What mechanism underlies this preference for a dimer-dimer pathway? To address this question, we explored the possibility that when a dimer forms, new sites are created that favor interactions with another dimer rather than with another monomer. These new association sites may not necessarily be the same as those mediating self-association of monomers in dimer formation. We propose that monomers form dimers and that dimers interact using distinctly different interaction sites to form tetramers. Having demonstrated that tandem dimers are translated completely and are stable, we could use these constructs to explore the possibility that monomers and dimers provide different interaction sites for subsequent oligomerization to form the channel tetramer. We assume that a tandem dimer, because its subunits are covalently linked, once translated, will rapidly fold into a dimer protein that is conformationally competent for oligomerization. This assumption is well supported by the recent work of Liu et al. (1998), which showed for cyclic nucleotide-gated channels, close relatives of voltage-gated $K^+$ channels, that 1) the subunits within a tandem dimer preferentially associate with each other, and 2) the tetrameric channel is composed of two functional dimers.

The strategy used to indicate whether monomers and dimers have different interaction sites was the following. We compared whether currents derived from expression of a WT monomer or a tandem dimer could be suppressed by coexpression with a Kv1.3 peptide fragment. We used this strategy previously to locate potential intersubunit interaction sites in Kv1.3 (Tu et al., 1996; Sheng et al., 1997). First, however, it was necessary to characterize the time course of current expression from monomer and tandem dimer cRNA under the conditions of the suppression experiments (3–15 ng/oocyte). This was important because to compare the potency of suppressors, we had to ensure that the experiments were carried out for comparable expression levels of channels derived from monomer and from tandem dimer. Current levels were maximal at similar times within the postinjection period studied (15–50 h). When expression levels increased or decreased over this period, they did so as

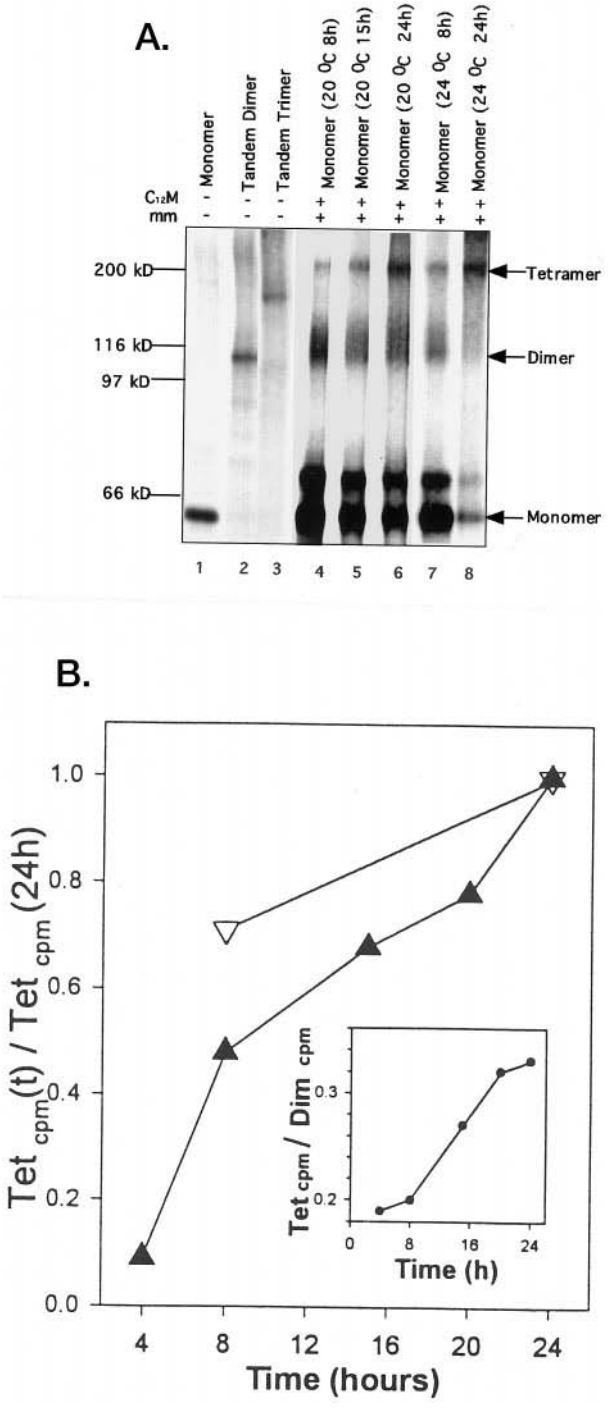


FIGURE 6 Nondenaturing gel electrophoresis of WT Kv1.3 in vitro translation products labeled with [$^{35}$S]methionine. (*A*) Lanes 1–3 contain translation products from in vitro translation of cRNA for WT monomer, WT-WT tandem dimer, and WT-WT-WT tandem trimer, respectively, in the absence of microsomal membranes (−mm) and solubilized in sampling buffer (0.1% SDS, no dithiothreitol (DTT)). Lanes 4–6 and 7–8 contain products from translation of WT monomer in microsomal membranes (+mm; 1.8 $\mu$l/25 $\mu$l rabbit reticulocyte lysate) at 20°C and 24°C, respectively, for the indicated times. Samples were pelleted through a sucrose cushion (Sheng et al., 1997) in the absence of DTT; solubilized in buffer containing 100 mM sodium phosphate, 5 mM KCl, 1% $C_{12}$M (dodecylmaltoside; Anatrace, Maumee, OH), pH 7.0, for 45 min at 4°C; diluted with sampling buffer (0.1% SDS, no DTT); and loaded on the gel (7.5% PAGE) without heating. Lanes 4–6 were loaded with equal sample volumes; lanes 7 and 8 were loaded with equal sample volumes. In lane 8 decreased total protein with time is likely due to aggregation, which is manifested in the stacking gel (data not shown). The bands at ~70 kDa in lanes 4–8 are background bands derived from the translation system. (*B*) The ratio of tetramer cpm to tetramer cpm at 24 h is plotted for in vitro translations at 20°C (▲) and 24°C (▽) for the indicated times for experiments as in *A*. (*Inset*) The ratio of tetramer cpm to dimer cpm for the indicated times for the 20°C experiments in *B*. Quantitation of the gels was carried out directly with a Molecular Dynamic PhosphoImager.

a function of the batch of oocytes, not as a function of the construct. Current derived from either monomer or tandem constructs increased or decreased similarly and simultaneously, i.e., the relative current amplitudes were independent of time.

The peptide fragment S1-S2-S3 is a strong suppressor of Kv1.3 (Tu et al., 1996; Sheng et al., 1997). Fig. 7 shows that S1-S2-S3 suppressed current by 60% compared to a CD4 control (Tu et al., 1996) when coexpressed with Kv1.3 WT monomer, but only by 18% when coexpressed with the tandem dimer. Strong suppression was observed even when the mole ratio of WT monomer:S1-S2-S3 was 1:1, and no significant suppression occurred even when the mole ratio of tandem dimer:S1-S2-S3 was 1:4 (data not shown). In contrast, S3-S4-S5, another strong suppressor (Tu et al., 1996), suppressed the median current derived from both WT monomer and WT-WT tandem dimer by 41% ($n = 8$) and 48% ($n = 8$), respectively. These results suggest that monomer and dimer may have different sensitivities to suppressor peptides, which may reflect different suppression sites in the monomer versus the dimer. Further support for this proposition is the differential suppression of current for the coexpression of another suppressor, a chimeric monomer composed of Kv1.3 ($NH_2$ terminus through S1) and Kv3.1 (S2 through C terminus), with monomer versus with tandem dimer. The chimera itself does not produce current (0.17 ± 0.03 $\mu$A, $n = 6$), yet it produced a median suppression of 53% for WT monomer ($n = 6$, $p = 0.0043$), but a median suppression of only 9% ($n = 10$, $p = 0.623$) for tandem dimer (data not shown). Regardless of whether the mole ratio of channel precursor:chimera cRNA was 1:1 or 1:2, the chimera only suppressed current derived from the monomer (data not shown).

If monomers and dimers have different interaction sites, and dimer-dimer association is a major pathway in channel assembly, then current derived from either WT monomers or tandem dimers should be suppressed by AV-(WT-P). This will be true regardless of their different suppression sites. In the first case, WT monomers will self-associate to form a WT dimer, which will readily associate with AV-(WT-P). In the second case, WT tandem dimer also will readily dimerize with AV-(WT-P). As shown in Fig. 8, current derived from WT monomer was suppressed by 93%, and current derived from tandem dimer was suppressed by 78%. Based on a binomial distribution of tetramers formed from WT homodimers and AV-(WT-P) tandem dimers, this level of suppression is predicted for a AV-(WT-P):WT

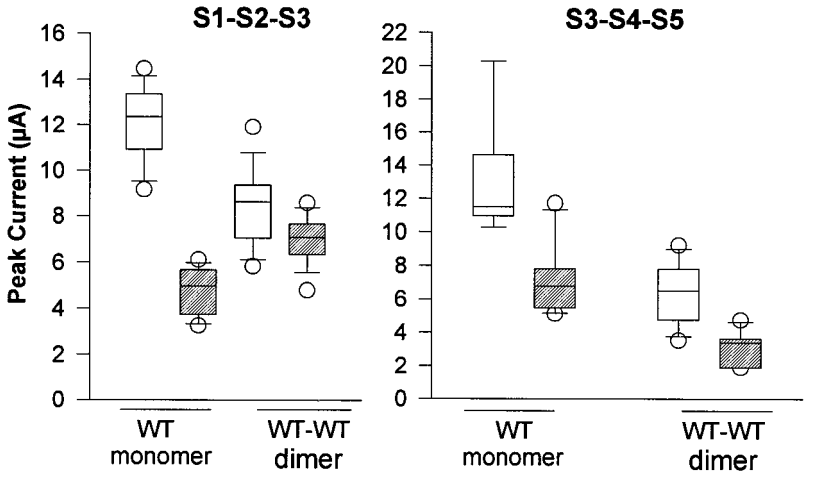


FIGURE 7 Effect of S1-S2-S3 and S3-S4-S5 on current expressed in oocytes from monomer and tandem dimer cRNA. Oocytes were coinjected with cRNA for WT and CD4 (control, *open symbols*), S1-S2-S3 (*shaded symbols*), or S3-S4-S5 (*shaded symbols*), or with cRNA for tandem dimer and either CD4 (control, *open symbols*), S1-S2-S3 (*shaded symbols*), or S3-S4-S5 (*shaded symbols*). The mole ratio of channel:suppressor cRNA was 1:2 (Tu et al., 1996). Recordings were made at 24 and 48 h postinjection and gave similar results. The peak current at +50 mV was measured. Data are represented as box plots. (For S1-S2-S3: $n = 8$ for monomer experiments, $n = 10$ for tandem dimer experiments. For S3-S4-S5: $n = 8$ for monomer experiments, $n = 6$ for tandem dimer experiments.) S1-S2-S3 and S3-S4-S5 each suppressed monomer-derived current ($p < 0.0001$ and $p = 0.030$, respectively; Mann-Whitney rank sum test), whereas only S3-S4-S5 suppressed dimer-derived current ($p = 0.008$; Mann-Whitney rank sum test).

cRNA mole ratio of 2:1. Strong suppression occurred for holding potentials of −140 and −100 mV.

Thus far, all constructs that suppressed current derived from tandem dimers also suppressed current derived from monomers; however, the reverse was not true. Because suppression sites may comprise a subset of intersubunit association sites (Tu et al., 1996; Sheng et al., 1997), we propose that monomer-monomer interactions occur to form dimers, using association sites different from those used in subsequent dimer-dimer interactions to form tetramers. Moreover, these differences may underlie the preferred dimer-dimer pathway in assembly.

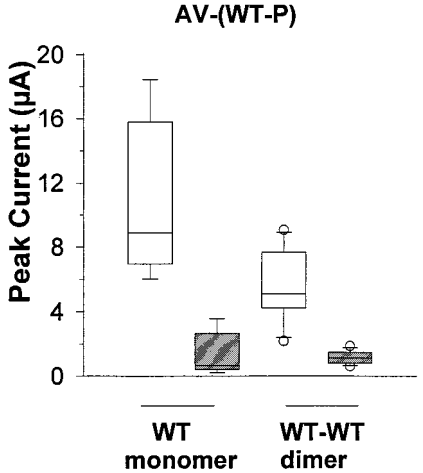


FIGURE 8 Effect of AV-(WT-P) on WT and WT-WT current expressed in oocytes. Oocytes were coinjected with cRNA for WT and either CD4 (control, *open symbols*) or AV-(WT-P) (*shaded symbols*), or with cRNA for WT-WT and either CD4 (control, *open symbols*) or AV-(WT-P) (*shaded symbols*). Conditions were the same as those for Fig. 7. Recordings were made at 24 and 48 h postinjection and gave similar results. Data are represented as box plots ($n = 8$ for monomer experiments; $n = 6$ for tandem dimer experiments). AV-(WT-P) suppressed WT current ($p = 0.008$; Mann-Whitney rank sum test) and WT-WT current ($p = 0.0007$; Mann-Whitney rank sum test).

## DISCUSSION

In this study we used a variety of techniques and strategies to assess the relative contributions of a sequential monomer addition pathway and a dimer-dimer pathway in the formation of a voltage-gated $K^+$ channel. Expression of functionally tagged tandem dimers and trimers demonstrated that dimeric interactions occur during oligomerization. Moreover, suppression experiments show that these dimeric interactions may be mediated by association sites different from those mediating monomer-monomer interactions, thus implicating conformational changes that accompany dimer formation. Regardless of the approach, our kinetic analysis suggests that the dimer-dimer pathway prevails in tetramer formation, even when the relative concentration of injected WT cRNA monomer is high (1:5 mole ratio of WT-AV:WT cRNA). In this case, the fraction of all channels formed by a dimer-dimer pathway is 1.0 ($w_d$, Table 2), and 69% of all channels made are homotetramers, indicating that synthesis of WT monomers is relatively high under these conditions. Yet the percentage of homotetramers that are made by the dimer-dimer pathway is close to 100%. Consistent with these results is the detection of dimers and tetramers, but not trimers, from the in vitro translation of WT monomers (Fig. 6).

A dimer-dimer pathway may be inferred from the stoichiometry of other $K^+$ channels. For instance, some isoforms produce functional channels only as 2:2 heterotetram-

ers (Jegla and Salkoff, 1997; Corey et al., 1998). And it has recently been shown that a highly stable tetrameric $K^+$ channel isolated from *Streptomyces lividans* can exist as a dimer (Cortes and Perozo, 1997). There is precedence for initial formation of stable dimers in the assembly of other types of channels. For example, dimers subsequently combine (along with a $\beta$-subunit) to form the final pentameric acetylcholine receptor channel (Gu et al., 1991; Saedi et al., 1991; Blount et al., 1990; however, see Green and Claudio, 1993). The influenza virus M2 protein is a homotetrameric channel formed by noncovalent association of monomers, stabilized by disulfide-linked dimers (Holsinger and Lamb, 1991; Sakaguchi et al., 1997). Similarly, many other viral membrane proteins from paramyxoviruses, lentiviruses, and a retrovirus form a tetramer by dimerization of dimers (for a review, see Doms et al., 1993). In some of these cases, the dimers are disulfide-linked, but the association between two dimers to form a tetramer is not mediated by covalent binding; in other cases, neither the dimers nor the tetramers are covalently linked. Another example is the T-cell antigen receptor. It is a complex of eight transmembrane proteins (Manolios et al., 1991) consisting of four dimers, which assemble via pairwise interactions. Only two of the dimers are disulfide-linked. Although disulfide links can be made between *Shaker* subunits (Schulteis et al., 1996), they are not necessary for the assembly of a functional *Shaker* $K^+$ channel, nor is there evidence that disulfide bonds exist in the final, tetrameric channel (Boland et al., 1994; Schulteis et al., 1995; Lu and Deutsch, unpub. data). However, it is not clear whether disulfide bonds facilitate assembly and/or enhance channel expression (Boland et al., 1994), or whether transient disulfide links stabilize Kv1.3 dimers, thereby favoring the dimer-dimer pathway in tetramer formation. More likely, dimerization in Kv1.3 assembly involves noncovalent interactions. Finally, cyclic nucleotide-gated channels behave functionally like two coupled dimers (Liu et al., 1998), and the conducting pore contains two identical titratable sites, each formed by two glutamates, each donated from diagonally opposed subunits in the tetramer (Root and MacKinnon, 1994). These findings support the possibility that dimers dimerize to form tetrameric channels.

We explored the kinetic implications of the apparent predominance of the dimer-dimer pathway by a simulation. Specifically, if $w_d$ is close to unity, what are the relative rate constants for each step in tetramer formation? The assembly of WT monomers may be represented by the following kinetic scheme (also see Appendix).

Simulation of tetramer formation for this model at steady state (Fig. 9) shows that $w_d$ values approach 1.0 only when the dimer-dimer pathway is strongly favored by the rate constants, for example, when $k_{11}$ and $k_{22}$ are relatively large, or when $k_{32} \gg k_{13}$. Fig. 6 shows that [Tri] $\ll$ [Dim], indicating either that the monomer addition pathway exists and the lifetime of the trimer is extremely short-lived ($k_{13}$ and $k_{32}$ are very large), or that the monomer addition pathway is rarely entered ($k_{22} \gg k_{12}$). The kinetic analysis (Fig. 5 and Table 2) favors the latter alternative.

Our finding that the dimer-dimer pathway is preferred in these experiments, especially as the relative amount of homotetramer increases, is intriguing. Although we have entertained several hypotheses for this trend, including the possibility that increasing monomer concentration catalyzes an increase in $k_{11}$, the observed increase in $w_d$ with increasing monomer synthesis suggests that the ER membrane is an important determinant of the oligomerization pathway in vivo. Restriction of membrane proteins in the two-dimensional plane of the ER membrane might serve to concentrate monomers and speed the kinetics of oligomerization (Helenius et al., 1992), thereby promoting the dimer-dimer pathway for efficient assembly of tetrameric membrane proteins.

The mechanisms whereby monomers form dimers and dimers subsequently dimerize to form tetramers are not known. To begin to address this issue, we tested the ability of two different Kv1.3 peptide fragments, which had previously been shown to suppress Kv1.3 current (Tu et al., 1996; Sheng et al., 1997), to suppress current derived from monomer or from tandem WT-WT dimer. This strategy has been used to identify candidates for inter- and/or intrasubunit association sites in Kv1.3. The fact that S1-S2-S3 and S3-S4-S5 both suppressed monomers, but only S3-S4-S5 suppressed tandem dimer, suggests that interaction sites between suppressors and dimers are different from those between suppressors and monomers. Thus the previously reported suppression of Kv1.3 ($T1^-$) (Tu et al., 1996; Sheng et al., 1997) by different Kv1.3 fragments might reflect suppression at different stages of oligomerization, for example, association of monomers to form dimers versus association of dimers to form tetramers. Whether these two suppressor peptides bind to different inter- and/or intrasubunit association sites remains to be proved. As shown by coimmunoprecipitation assays (Sheng et al., 1997), the mechanism of suppression of $K^+$ channel function by the transmembrane peptide fragments is due to direct physical association of the peptide fragment with $K^+$ channel pro-

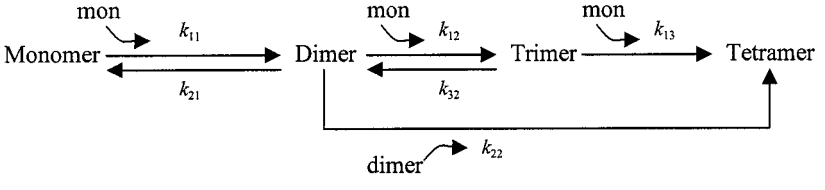


SCHEME III

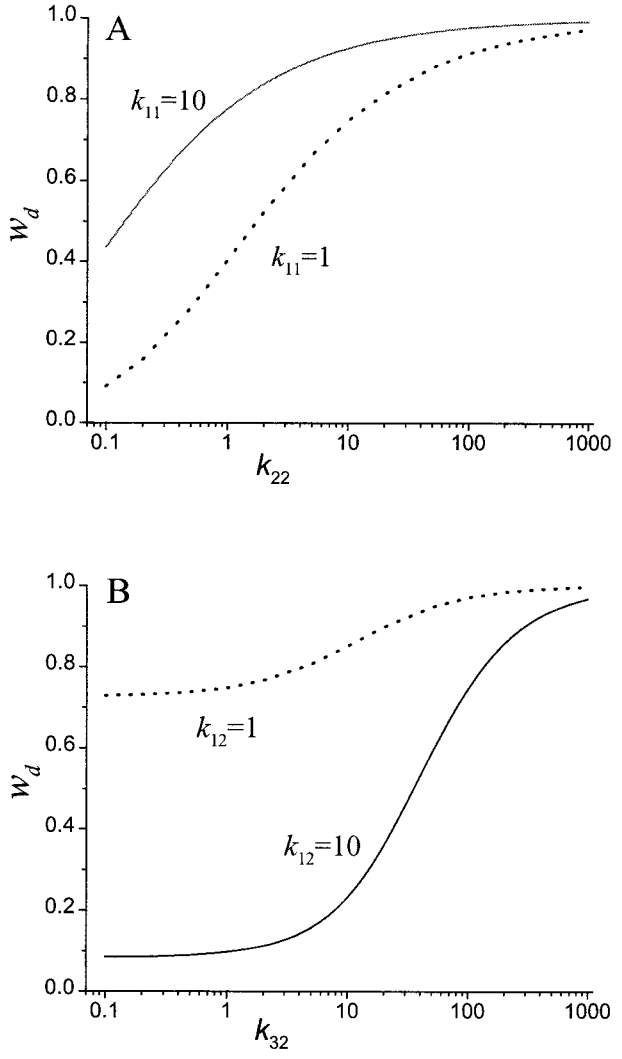


FIGURE 9 $w_d$ values from simulations of tetramer assembly from WT monomers. The model and equations are shown in the Appendix. All rate constants are presented in arbitrary units with respect to $k_{21}$, which had a value of unity. The rate of tetramer assembly was set at $T = 100$. After solving the steady-state equations for assembly (see Materials and Methods and the Appendix), $w_d$ was calculated as $k_{22}$[dimer]$^2/T$. (*A*) Effect of $k_{22}$ on $w_d$, for the indicated values of $k_{11}$. For this simulation $k_{12} = 1$, $k_{13} = 1$, and $k_{32} = 1$. (*B*) Effect of $k_{32}$ on $w_d$, for the indicated values of $k_{12}$. For this simulation $k_{11} = 1$, $k_{13} = 1$, and $k_{22} = 10$.

tein. Although similar studies would be very useful for investigating these putatively different interaction sites, in vitro experiments are currently difficult because of the low efficiency of cotranslated tandem dimers in vitro.

An additional implication comes from the observation that the chimera suppressed current derived from the monomer, but not current derived from the tandem dimer. It has been shown previously that a peptide fragment containing the $NH_2$ terminus and the first transmembrane segment of voltage-gated $K^+$ channels can specifically and potently suppress the parent channel (Tu et al., 1995; Babila et al., 1994). This $NH_2$ terminus contains a so-called T1 recognition domain (Shen et al., 1993; Li et al., 1992), which confers subfamily specificity in the assembly of voltage-gated $K^+$ channels (Xu et al., 1995). In the case of Kv1.3, T1 alone cannot suppress WT; however, a peptide containing both the $NH_2$ terminus and the first transmembrane-spanning segment can potently suppress WT (Tu et al., 1995). One interpretation of the suppression results is that T1 interactions prevail at the monomer-monomer association stage, and that other specific interactions govern dimer-dimer association to form tetramers.

A cartoon depicting the conformational changes that accompany dimerization of monomers is shown in Fig. 10. The notable features of this model are that monomers have interaction sites different from those of dimers, that dimerization of monomers creates new interaction sites, and that some monomers can still interact with dimers, albeit not as easily as dimers (i.e., $k_{22} \gg k_{12}$). A model that incorporates conformational changes in dimeric intermediates as a prerequisite for subsequent assembly steps is extremely attractive. Such a mechanism ensures a limited number of interacting monomers versus an unlimited string of monomers if a monomer binding site is continuously available.

## APPENDIX

Scheme II (Results) represents tetramer formation when oocytes are coinjected with cRNAs encoding WT monomer and a tandem heterodimer. The detailed kinetic model for Scheme II is shown as:

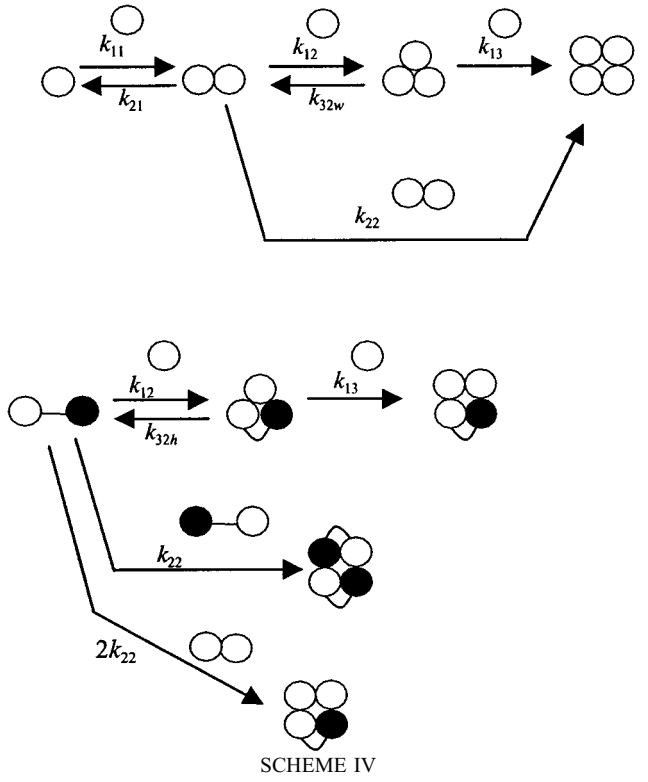


SCHEME IV

Notice that the dimer-dimer pathway is capable of synthesizing all three species of tetramer, whereas the monomer addition pathway cannot produce the 2:2 heterotetramer. At steady state, where the rates of monomer synthesis (*RM*) and heterodimer synthesis (*RD*) are assumed to be constant, the above kinetic model may be described as a set of eight coupled differential equations:

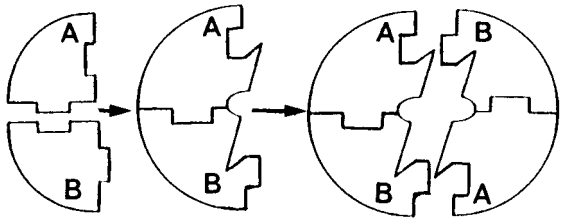


FIGURE 10 Cartoon model for the dimer-dimer pathway in the channel assembly. In the first step, two monomers form a dimer, thereby creating new interaction sites that did not exist in the prior monomer. In the second step, these new sites are used in the next stage to form tetramers.

$$RM = -\frac{d[Mon]}{dt} = k_{11}[Mon]^2 + k_{12}[Mon]([D_{wt}] + [D_{ht}]) + k_{13}[Mon]([Tr_{wt}] + [Tr_{ht}]) - (k_{21}[D_{wt}] + k_{32h}[Tr_{ht}] + k_{32w}[Tr_{wt}]) \quad (A1)$$

$$RD = -\frac{d[D_{ht}]}{dt} = k_{12}[Mon][D_{ht}] + k_{22}[D_{ht}](2[D_{wt}] + [D_{ht}]) - k_{32h}[Tr_{ht}] \quad (A2)$$

$$0 = -\frac{d[D_{wt}]}{dt} = k_{12}[Mon][D_{wt}] + k_{22}[D_{wt}]([D_{wt}] + 2[D_{ht}]) - k_{11}[Mon]^2 + k_{21}[D_{wt}] - k_{32w}[Tr_{wt}] \quad (A3)$$

$$0 = -\frac{d[Tr_{wt}]}{dt} = k_{13}[Mon][Tr_{wt}] - k_{12}[Mon][D_{wt}] + k_{32w}[Tr_{wt}] \quad (A4)$$

$$0 = -\frac{d[Tr_{ht}]}{dt} = k_{13}[Mon][Tr_{ht}] - k_{12}[Mon][D_{ht}] + k_{32h}[Tr_{ht}] \quad (A5)$$

$$S_{4:0} = \frac{d[Tet_{4:0}]}{dt} = k_{13}[Mon][Tr_{wt}] + k_{22}[D_{wt}]^2 \quad (A6)$$

$$S_{3:1} = \frac{d[Tet_{3:1}]}{dt} = k_{13}[Mon][Tr_{ht}] + 2k_{22}[D_{wt}][D_{ht}] \quad (A7)$$

$$S_{2:2} = \frac{d[Tet_{2:2}]}{dt} = k_{22}[D_{ht}]^2 \quad (A8)$$

The concentration of each species is in square brackets. The WT monomer is *Mon*; the WT dimer is $D_{wt}$; the heterodimer is $D_{ht}$; the WT trimer is $Tr_{wt}$; the 2:1 heterotrimer is $Tr_{ht}$; the 4:0 homotetramer is $Tet_{4:0}$; the 3:1 tetramer is $Tet_{3:1}$; and the 2:2 tetramer is $Tet_{2:2}$. The rates of tetramer formation are given as $S_{i:j}$, where i:j represents the number of WT and mutant subunits in the tetramer, respectively. The total rate of tetramer synthesis is

$$T = S_{4:0} + S_{3:1} + S_{2:2}.$$

This model assumes that forward rate constants are insensitive to the A413V mutation (*filled circles*) and to the tandem constructs. For generality, however, we have allowed the dissociation of trimers to be dependent on subunit composition, because the dissociation of a monomer from a tandem construct is not possible.

Finally, note that the rates of forming tetramers from two dimers are twofold greater when the reactant species are different than when they are the same. This is a statistical factor derived from the kinetic theory of collisions between molecules (Moore, 1972).

In the case of expression of WT monomers, the above model reduces to a set of four equations by removing all species associated with the tandem construct. These equations were used to calculate $w_d$ in Fig. 9.

We thank Jing Wang and Vincent Santarelli for technical assistance. We thank Dr. J. Patlak for his careful reading of the manuscript and Dr. C. Miller for his scrupulously critical evaluation of the manuscript and for rescuing us from the abyss. And special thanks to Dr. Spike Horn for his insights and substantial contribution to the analysis and computer programming aspects of this project.

This work was supported by National Institutes of Health grants GM 52302, HL 07027-24, and TW00722.

## REFERENCES

Babila, T., A. Moscucci, H. Wang, F. E. Weaver, and G. Koren. 1994. Assembly of mammalian voltage-gated potassium channels: evidence for an important role of the first transmembrane segment. *Neuron.* 12:615–626.

Blount, P., M. M. Smith, and J. P. Merlie. 1990. Assembly intermediates of the mouse muscle nicotinic acetylcholine receptor in stably transfected fibroblasts. *J. Cell Biol.* 111:2601–2611.

Boland, L. M., M. E. Jurman, and G. Yellen. 1994. Cysteines in the Shaker $K^+$ channel are not essential for channel activity or zinc modulation. *Biophys. J.* 66:694–699.

Busch, A. E., R. S. Hurst, R. A. North, J. P. Adelman, and M. P. Kavanaugh. 1991. Current inactivation involves a histidine residue in the pore of the rat lymphocyte potassium channel RGK5. *Biochem. Biophys. Res. Commun.* 179:1384–1390.

Chahine, M., L. Chen, R. L. Barchi, R. G. Kallen, and R. Horn. 1992. Lidocaine block of human heart sodium channels expressed in *Xenopus* oocytes. *J. Mol. Cell. Cardiol.* 24:1231–1236.

Corey, S., G. Krapivinsky, L. Krapivinsky, and D. E. Clapham. 1998. Number and stoichiometry of subunits in the native atrial G-protein-gated $K^+$ channel, $I_{KACh}$. *J. Biol. Chem.* 273:5271–5278.

Cortes, D. M., and E. Perozo. 1997. Structural dynamics of the *Streptomyces lividans* $K^+$ channel (SKC1): oligomeric stoichiometry and stability. *Biochemistry.* 36:10343–10352.

Deal, K. K., D. M. Lovinger, and M. M. Tamkun. 1994. The brain Kv1.1 potassium channel: in vitro and in vivo studies on subunit assembly and posttranslational processing. *J. Neurosci.* 14:1666–1676.

Doms, R. W., R. A. Lamb, J. K. Rose, and A. Helenius. 1993. Folding and assembly of viral membrane proteins. *Virology.* 193:545–562.

Doyle, D. A., J. M. Cabral, R. A. Pfuetzner, A. L. Kuo, J. M. Gulbis, S. L. Cohen, B. T. Chait, and R. MacKinnon. 1998. The structure of the potassium channel: molecular basis of $K^+$ conduction and selectivity. *Science.* 280:69–77.

Green, W. N., and T. Claudio. 1993. Acetylcholine receptor assembly: subunit folding and oligomerization occur sequentially. *Cell.* 74:57–69.

Gu, Y., J. R. Forsayeth, S. Verrall, X. Yu, and Z. W. Hall. 1991. Assembly of mammalian muscle acetylcholine receptors in transfected COS cells. *J. Cell Biol.* 114:799–807.

Heginbotham, L., and R. MacKinnon. 1992. The aromatic binding site for tetraethylammonium ion on potassium channels. *Neuron.* 8:483–491.

Helenius, A., T. Marquardt, and I. Braakman. 1992. The endoplasmic reticulum as a protein-folding compartment. *Trends Cell Biol.* 2:227–231.

Holsinger, L. J., and R. A. Lamb. 1991. Influenza virus M2 integral membrane protein is a homotetramer stabilized by formation of disulfide bonds. *Virology.* 183:32–43.

Jegla, T., and L. Salkoff. 1997. A novel subunit for Shal $K^+$ channels radically alters activation and inactivation. *J. Neurosci.* 17:32–44.

Li, M., Y. N. Jan, and L. Y. Jan. 1992. Specification of subunit assembly by the hydrophilic amino-terminal domain of the Shaker potassium channels. *Science.* 257:1225–1230.

Li, M., N. Unwin, K. A. Stauffer, Y. Jan, and L. Y. Jan. 1994. Images of purified Shaker potassium channels. *Curr. Biol.* 4:110–114.

Liu, D. T., G. R. Tibbs, P. Paoletti, and S. A. Siegelbaum. 1998. Constraining ligand-binding site stoichiometry suggests that a cyclic nucleotide-gated channel is composed of two functional dimers. *Neuron.* 21:235–248.

Liu, D. T., G. R. Tibbs, and S. A. Siegelbaum. 1996. Subunit stoichiometry of cyclic nucleotide-gated channels and effects of subunit order on channel function. *Neuron.* 16:983–990.

MacKinnon, R. 1991. Determination of the subunit stoichiometry of a voltage-activated potassium channel. *Nature.* 350:232–235.

Manolios, N., F. Letourneur, J. S. Bonifacino, and R. D. Klausner. 1991. Pairwise, cooperative and inhibitory interactions describe the assembly and probable structure of the T-cell antigen receptor. *EMBO J.* 10: 1643–1651.

McCormack, K., L. Lin, L. E. Iverson, M. A. Tanouye, and F. J. Sigworth. 1992. Tandem linkage of Shaker $K^+$ channel subunits does not ensure the stoichiometry of expressed channels. *Biophys. J.* 63:1406–1411.

Moore, W. J. 1972. Physical Chemistry, 4th Ed. Prentice Hall, Englewood Cliffs, NJ. 150.

Nagaya, N., and D. M. Papazian. 1997. Potassium channel a and b subunits assemble in the endoplasmic reticulum. *J. Biol. Chem.* 272:3022–3027.

Ogielska, E. M., W. N. Zagotta, T. Hoshi, S. H. Heinemann, J. Haab, and R. W. Aldrich. 1995. Cooperative subunit interactions in C-type inactivation of K channels. *Biophys. J.* 69:2449–2457.

Panyi, G., and C. Deutsch. 1996. Assembly and suppression of endogenous Kv1.3 channels in human T cells. *J. Gen. Physiol.* 107:409–420.

Panyi, G., and C. Deutsch. 1997. Anomalous inactivation of a Kv1.3 mutant. *Biophys. J.* 72:A27.

Panyi, G., Z. Sheng, L. Tu, and C. Deutsch. 1995. C-type inactivation occurs by a cooperative mechanism. *Biophys. J.* 69:896–904.

Root, M. J., and R. MacKinnon. 1994. Two identical noninteracting sites in an ion channel revealed by proton transfer. *Science.* 265:1852–1856.

Saedi, M. S., W. G. Conroy, and J. Lindstrom. 1991. Assembly of *Torpedo* acetylcholine receptors in *Xenopus* oocytes. *J. Cell Biol.* 112: 1007–1015.

Sakaguchi, T., Q. Tu, L. H. Pinto, and R. A. Lamb. 1997. The active oligomeric state of the minimalistic influenza virus M2 ion channel is a tetramer. *Proc. Natl. Acad. Sci. USA.* 94:5000–5005.

Schulteis, C. T., S. A. John, Y. Huang, C. Tang, and D. M. Papazian. 1995. Conserved cysteine residues in the Shaker $K^+$ channel are not linked by a disulfide bond. *Biochemistry.* 34:1725–1733.

Schulteis, C., N. Nagaya, and D. Papazian. 1996. Intersubunit interaction between amino- and carboxy-terminal cysteine residues in tetrameric Shaker $K^+$ channels. *Biochemistry.* 35:12133–12140.

Shen, N. V., X. Chen, M. M. Boyer, and P. Pfaffinger. 1993. Deletion analysis of $K^+$ channel assembly. *Neuron.* 11:67–76.

Sheng, Z., W. Skach, V. Santarelli, and C. Deutsch. 1997. Evidence for interaction between transmembrane segments in assembly of Kv1.3. *Biochemistry.* 36:15501–15513.

Tu, L., V. Santarelli, and C. Deutsch. 1995. Truncated $K^+$ channel DNA sequences specifically inhibit Kv1.3 and Kv3.1 expression in mouse T lymphocytes. *Biophys. J.* 68:147–156.

Tu, L., V. Santarelli, Z.-F. Sheng, W. Skach, D. Pain, and C. Deutsch. 1996. Voltage-gated $K^+$ channels contain multiple intersubunit association sites. *J. Biol. Chem.* 271:18904–18911.

Xu, W. Y., J. N. Jan, L. Jan, and M. Li. 1995. Assembly of voltage-gated potassium channels. Conserved hydrophilic motifs determine subfamily-specific interactions between the a-subunits. *J. Biol. Chem.* 270: 24761–24768.